ATOLL RESEARCH BULLETIN

NO. 408

CHAPTER 10

HYDRODYNAMIC OBSERVATIONS OF THE COCOS (KEELING) ISLANDS LAGOON

BY

P. KENCH

ISSUED BY
NATIONAL MUSEUM OF NATURAL HISTORY
SMITHSONIAN INSTITUTION
WASHINGTON, D.C., U.S.A.
FEBRUARY 1994

CHAPTER 10

HYDRODYNAMIC OBSERVATIONS OF THE COCOS (KEELING) ISLANDS LAGOON

BY

P. KENCH *

INTRODUCTION

Atoll lagoon hydrodynamic studies to date have primarily focused on the mass flux of water and nutrients through lagoon systems and identified the principle driving mechanisms of lagoon circulation and flushing (von Arx 1948, 1954, Gallagher et al. 1971, Stroup and Meyers 1974, Smith and Jokiel 1978, Atkinson et al. 1981, Gilmour and Colman 1990).

In general, lagoon circulation has been found to respond to three driving mechanisms: wind-driven set-up on the windward ocean reef; wind stress on the lagoon surface, and tides (Atkinson et al. 1981, Andrews and Pickard 1990). Wind has been identified as the the primary driving mechanism of lagoon circulation in deeper lagoon systems (e.g. Bikini Atoll - 60m deep, von Arx 1954, Enewetak Atoll- 50 m deep, Atkinson 1981). Wind is not, however, thought to play a large role in the exchange of water between lagoon and ocean. In shallow lagoons such as that of Fanning Atoll (5 m) tidal forces are found to dominate both lagoon circulation and lagoon-ocean water exchange (Stroup and Meyers 1974).

The degree to which a lagoon is dominated by wind or tidal forces is found to depend on the lagoon depth and the degree of connection between the lagoon and open ocean (Wiens 1962, Stroup and Meyers 1974). The speed of lagoon-ocean exchange is also reliant upon the 'openness' of the lagoon with the ocean.

The majority of atoll hydrodynamic studies have been performed in the Pacific Ocean within deeper lagoons (50-60 m, Enewetak, Bikini lagoons) with the exception of the shallow Fanning Atoll lagoon (5m). There has been little research on the hydrodynamic processes within Indian Ocean atolls, except for research on the tidal characteristics of several atolls in the Western Indian Ocean (Farrow and Brander 1971, Pugh 1979, Pugh and Rayner 1981).

This paper describes results from the examination of the hydrodynamic processes of the lagoon of the Cocos (Keeling) Islands, in the eastern Indian Ocean (Fig. 1). It has three aims: first, to describe the tidal regime of the Cocos atoll lagoon; second, to examine the water currents and circulation within the lagoon and connections between the lagoon and ocean; and third, to establish the flushing characteristics of the atoll.

* Department of Geography and Oceanography, Australian Defence Force Academy, Canberra, Australian Capital Territory, 2601.

FIELD LOCATION

The main lagoon of the Cocos (Keeling) Islands is enclosed by 26 islands and has a surface area of 190 km^2. The lagoon can be divided into two distinct morphological zones: a deep (8-12 m) northern portion and a large shallow (0-3 m) southern region (Fig. 1). A network of deep blue holes exists in this shallow region with depths in excess of 20m. The lagoon opens to the northwest and northeast either side of Horsburgh Island where passes are deep (12-14 m) and wide (2-5 km). Eleven shallow passages (<2 m) connect the ocean and reef to the lagoon on the eastern and southern sides of the atoll.

The atoll is dominated by the southeast trade winds which prevail for most of the year. The islands also lie within the equatorial (westward flowing) ocean current (Neumann 1968), which reaches a maximum velocity of more than 1 knot (Tchernia 1980). In the northern hemisphere winter, movement of the Inter Tropical Convergence Zone (ITCZ) south of the equator produces variable winds and the Equatorial Counter Current (eastward flowing) may develop. The degree to which the Cocos (Keeling) Islands are affected by this counter current is dependent upon the extent of southward migration of the ITCZ (Neumann 1968).

The closest amphidromic point to the Cocos (Keeling) Islands is situated off the southwest coast of Australia (Platzman 1984, for the M_2 tide). The anti-clockwise rotation of the tidal wave around this point and the location of the Cocos (Keeling) Islands, suggest the tidal wave sets from the east-northeast.

METHODS

A field measurement program was undertaken from November 1991 to January 1992. Tidal observations have been taken on Cocos, by the Australian CSIRO Oceanography Division since 1963, from a permanent tide gauge on Home Island jetty (Fig. 1). For the duration of the field measurement period a temporary pressure tide gauge was deployed in the south of the atoll (Fig. 1) to identify any changes in tidal characteristics between the northern (deep) and southern (shallow) regions of the lagoon. This gauge operated successfully for 20 days before being fouled by marine algae. The permanent tide gauge was inoperative during the period of measurement by the temporary gauge. This limits direct comparison of observed elevation and time data. A harmonic analysis (Foreman 1979a) of water level observations from November 17 to December 6 (temporary gauge), and from March to April 1988 (permanent tide gauge) has been made to resolve the major tidal constituents at each location (ease of access to permanent tide gauge data being the primary factor deciding the period analysed).

Current speeds and directions were obtained using five bidirectional electromagnetic current metres. These metres were deployed for 16 day periods in 7 shallow passages and 5 sites within the lagoon (Fig. 1). Current metres were mounted 0.4 m above the bed in the passages and 0.5 m above the bed in the lagoon. Additional, shorter records (1-2 day) were obtained from the deeper passages to the northwest and northeastern sections of the lagoon, and from one station in the middle of the lagoon (Fig. 1). For these experiments 3 current metres were deployed vertically, at depths of 2 m below the surface, mid-depth and 1m above the bed. Current records, in all sampling periods, were 1 minute averages of current velocity taken at 10 minute intervals.

Current time series have been harmonically analysed to resolve the major tidal current constituents (Foreman 1979b). Constituents resolved for each time series were used to predict the tidal currents for the period analysed. Predicted currents were then subtracted from the observed current data to identify those components of the current record not attributed to tidal forces. These currents are termed 'residual currents'.

Velocity profiling using an impellor current metre was undertaken during neap and spring tidal conditions in all shallow passages. Velocity measurements at stations across each channel were corrected to 20 minute intervals and the cross-sectional area of each channel identified for each time increment. Cross-sectional area discharge relationships were then derived for each shallow passage.

Tidal prism - the volume of water entering and leaving the lagoon during a tidal cycle -was calculated for a 1m and 0.4m spring and neap tide respectively. Bathymetric charts (1983) provided lagoon depths relative to 0.7m below Mean Sea Level, corresponding to zero on the Home Island tide gauge. The surface area of the lagoon at low and high tide was estimated through planimetric analysis. The change in depth (1m-spring; 0.4m-neap) was then applied to the respective low and high tide surface areas to calculate the volume of the lagoon. Differences between high and low tide lagoon volumes provide estimates of tidal prisms for the neap and spring tides. With an estimation of total lagoon tidal prism, the contribution of shallow passage water flux to lagoon flushing is identified, and the ocean lagoon exchange time calculated.

RESULTS

Tides

Harmonic analysis of the tidal records identify the semi-diurnal constituents of greatest importance (Table 1) with the M_2 and S_2 constituents having amplitudes of 29 and 14 cm in the north of the lagoon and 25 and 5.6 cm in the south of the lagoon. These amplitudes also display a marked attenuation from north to south within the lagoon. The K_1 constituent has an amplitude of 12.19 cm and 10.28 cm for the north and southern parts of the atoll respectively (Table 1).

The southern lagoon tides lag those of the northern lagoon (Table 1). This lag is evident in the tidal records with observed high tides lagging those in the north by 15-55 minutes dependent on the tidal range and regime (spring or neap tides). Shallow water tides (M_4) are much larger in the shallow southern region of the atoll than the deeper northern lagoon.

The form of the tides as identified by the amplitude ratio $[F = (K_1 + O_1)/(S_2 + M_2)]$ is 0.44. This describes the tides as mixed mainly semi-diurnal. These tides characteristically have large inequalities in range and time between the highs and lows each day (Pond and Pickard, 1983). Mean spring tidal ranges using the equation $S = 2(M_2 + S_2)$ are 87 cm and 61.2 cm for the north and south of the atoll. These amplitudes display a marked attenuation of the tide from north to south. The analysis also identifies a 6.02 cm (north) and 7.21 cm (south) increase in Mean Sea Level between neap and spring tide conditions (Msf constituent, Table 1).

Current Circulation

Progressive vector plots of current information are shown in Figures 2-5 for forty-eight hour periods during neap and spring tides. Distance between the 6.5 hour increments allow comparison of the relative velocity and/or duration of tidal flow to be made between stations.

Lagoon

In all areas of the lagoon, except for the western shoreline, currents appear to be tidally modulated during both neap and spring tides (Figs. 2 and 3). The western shoreline of the lagoon exhibits a unidirectional northwestward flow throughout the rising and falling of the tide.

In the eastern part of the lagoon the net flow westward, during neap tides (Fig. 2), is indicative of the longer duration or faster velocity of the westward flowing ebb currents. This pattern changes during spring tidal conditions to a net movement to the northwest (Fig. 3). The southeastward rising tide current is however more prominent during spring tides and penetrates the lagoon to within 1 km of the lagoon shoreline of the eastern islands.

In the southeast of the lagoon net current movement is toward the southwest (neap tides) and west (spring tides). Westward drift is reduced during spring tidal conditions due to the greater oscillation of rising and falling tide currents in the southeast and northwestward directions (Fig. 3).

Current patterns in the southwest lagoon are similar for both the neap and spring tidal conditions. There is a net movement northwestward throughout the 48 hour period displayed. It is evident that rising tide currents penetrate south to within 1 km of the southern passage.

Tidal elevation plays an important role in the magnitude and time period of current reversal in the east and southeast sections of the lagoon. Comparisons of the neap and spring tidal currents identify a greater net movement of water during neap tidal conditions as shown by the distance between starting and finishing points of each 48 hour period. Net flow direction in the east and southeastern sectors of the lagoon rotate 45^{o} toward north during spring tide conditions. This highlights the increased importance of the south/north tidal flow on current direction during spring tides.

Current measurements taken at the deep northeastern passage (Fig. 2) convey a tidally modulated reversal in direction between the ocean and lagoon. This is accompanied by a net movement to the west. Measurements taken in the northwest passage, however, display a unidirectional flow to the southwest. This movement is hard to interpret. There appears to be no marked reversal of current direction with the oscillation of the tide and the direction seems to suggest water is leaving the lagoon. These currents are weak (5-10 cm/s)when compared to those of the northeastern passage. Measurements taken at mid-depth and 1m above the sea bed display similar current patterns to those shown by the surface current record in the deeper passages. Currents in the mid-lagoon are weak (0-7 cm/s) and appear to oscillate with the rising and falling tide (Fig. 2).

Shallow Passages

The shallow passages display a unidirectional flow from ocean-side reef to lagoon during neap tide conditions (Fig. 4). During spring tides the southern passages maintain the unidirectional flow (Fig. 5), while the eastern passages display a reversal in flow direction around low tide (Fig. 5). Due to the intertidal nature of the eastern passages at spring low tide the current record is broken causing distortion to the observed pattern. It is however clear that currents do travel from lagoon to ocean for part of the spring tidal cycle in the eastern passages.

Tidally Driven Currents

As tidal currents vary in speed their direction rotates, usually with a semi-diurnal period dominating (Pond and Pickard 1983). The figure traced out by the tip of a vector representing the tidal current will be an ellipse. Tidal current constituents are presented in Table 2 as properties of tidal current ellipses for the M_2 and K_1 constituents. Figure 6 presents the physical appearance of the M_2 tidal ellipses within the lagoon and shallow passages.

Lagoon currents are dominated by the M_2 tidal constituent (Table 2, Fig. 6) which is strongest in the southwest section of the lagoon at 16.95 cm/s. This constituent is also strong in the eastern side of the atoll at 11.36 cm/s. While the K_1 currents are the second strongest, they are much weaker than the M_2 currents ranging between 0.77cm/s and 4.84cm/s. M_3 and M_4 constituents (not listed) are the next strongest but are generally less than 1 cm/s. The narrow M_2 current ellipses in the east and southwestern sections of the lagoon (Fig. 6) reveal the strong oscillatory nature of tidal currents in these zones which are enhanced by the shallow passage flow. The small and wide ellipse of the southeastern lagoon portrays the weaker currents experienced in this zone. The shallow nature of this area and the curvature of South Island may contribute to the observed weak currents and direction of net flow to the west.

The M_2 currents in the southeast section of the lagoon have a phase lead over the eastern and southwestern areas of the lagoon. The K1 constituent, however, shows a phase lead of 5^{o} in the east of the lagoon followed by the southwestern section of the lagoon, with the southeastern portion lagging the east by 13^{o}. This lag may reflect the location of the current metre in the wide shallow western section of the lagoon causing shoaling of the tide. This is supported by the shallow water constituent (M4) having its largest magnitude in this zone (2.2 cm/s).

As with the lagoon currents, the shallow passage tidal currents are dominated by the M_2 tide which is strongest in the southern passages at 7.6 cm/s. The K_1 constituent is of secondary strength within the passages (Table 2).

Residual currents are those components of the observed currents that cannot be explained through gravitational tidal forces. They are produced by wind stress, wind waves and or internal waves (i.e. temperature or pressure gradients). Analysis of lagoon currents identifies a mean of 15.6% of observed currents that are produced by these 'other' forces (Table 2 and Figs. 7a and 7b). Within the lagoon residual currents have their greatest magnitude in the southeast lagoon where 17.2% of the northing component and 27% of the easting component not driven by tidal forces (Table 2). Residual currents account for up to 52% of the observed shallow passage currents. This explains the small semi-major axes lengths of the M_2 ellipses within the passages (Fig. 6), with residual currents being twice as strong as the M_2 tidal current. The orthogonal with the greatest residual strength coincides with the orientation of the passage, i.e. in the southern passages the residual current is greatest for the north-south component of velocity (Table 2 and Fig. 7c).

Figures 7a, b and c show the observed and residual current data for locations within the southeast and southwest regions of the lagoon and the southern passage. Apart from the first four days of observations within the southeast section of the lagoon the residual easting component currents flow to the west (Fig. 7a). It is suggested that residual currents in this section of the lagoon are driven by the southeast trade winds. The strength of the residual current would, therefore, depend on wind strength. Residual currents in the southwest section of the lagoon (Fig. 7b) appear to fluctuate with tidal elevation. The magnitude of these currents is small. The large node in the southern passage residual current (Fig. 7c), coincides with tropical cyclone activity that influenced the island from December 5-8, 1991. The marked velocity increase, may have been the result of increased wave action and tidal elevation at the reef crest together with increased wind speeds. Correlation of wind strength and direction, and current direction, is required to identify the driving mechanisms of the residual currents.

Shallow Passage Water Flux, Tidal Prisms and Lagoon Exchange

Lagoon tidal prisms calculated for a 1m (spring) and 0.4m (neap) tide are presented in Table 3. The spring tidal prisms for each shallow passage are shown in Figure 8 and cumulative spring and neap prisms for the shallow passages are presented in Table 3. A relationship is found between the cross-sectional area of each passage and the tidal prism, with larger passages transmitting greater volumes of water from ocean to lagoon (Fig. 8).

On the rising spring tide the shallow passages contribute 10% to the tidal prism. The deeper passages to the north and northeast therefore must transmit 90% of the rising spring tide prism. During the falling tide shallow passages still transmit water from the ocean to the lagoon (approximately 50% of the flood tide contribution). Over a full tidal cycle, therefore, the shallow passages contribute 14% of the total spring tidal prism. Invoking a neap tidal range of 0.4 m the rising tide prism is much smaller than the spring tide prism (Table 3). The shallow passages contribute 16.9% to the neap rising tide prism. Over an entire tidal cycle the contribution of the shallow passages to the prism is proportionately much greater than it is for spring tides (22%).

In calculating the flushing time of the lagoon several assumptions have been made. First, the volume of water that enters the lagoon during the rising tide equals that leaving the lagoon during the falling tide. Water entering the lagoon through the shallow passages during the falling tide, will however, be retained within the lagoon. The semi-diurnal nature of the tidal regime would also result in more water being retained in the lagoon if the low tide did not equal the original tide level. Second, the falling tide prism expels water that resided in the lagoon at low tide. With these assumptions it requires a minimum of 2.36 days (spring tide) and 5.54 days (neap tide) for the lagoon to exchange its volume with the ocean.

DISCUSSION

It is evident that the Cocos (Keeling) Islands lagoon experiences mixed semi-diurnal tides with a marked diurnal inequality (Table 1). The spring tidal range in the north of the lagoon of 0.82 m, although higher than most central Pacific atolls, falls within the lower range of Indian Ocean tidal ranges (Farrow and Brander 1971) and is considerably less than the 2.74m experienced at Aldabra atoll. A phase lag is identified within the lagoon; with the tide in the south of the atoll lagging the north. This phase lag is also manifested in the tidal current properties for the K_1 currents (Table 2). Southern passage M_2 currents lag those of the eastern passages by 111°. This evidence supports the tidal lag relationship, suggesting that the tide sets from the east-northeast and travels south through the lagoon.

Attenuation of tide heights was observed from north to south within the lagoon but due to the short length of data in the south of the atoll (20 days) it is not appropriate to place great significance on these differences. The broad, shallow nature of the southeastern section of the lagoon is responsible for the significant shallow water effects (M_4 constituent) in this region. Shallow water effects were identified by Pugh and Rayner (1981) in Salomon atoll, which they attributed to the more enclosed nature of the lagoon.

Pugh and Rayner (1981) highlighted the importance of an atoll's tidal characteristics in contributing to the ecological behaviour of reef systems. Farrow and Brander (1971) established that the timing of extreme low water at Aldabra Atoll was synchronous with maximum solar radiation. This was thought to maximise stress on many organisms on the reef. Within the Cocos lagoon the maximum exposure of reef flats occurred at midnight with the second, higher low-tide of the day occurring around midday. Reef organisms were, therefore, not stressed by solar radiation during the most extreme low tide levels.

Lagoon currents and circulation are driven by the tidal regime (Table 2, Figs 2 and 3), with rising tide currents penetrating south into the lagoon within 1km of the eastern and southern passages. The component of observed currents not attributable to tidal forces, may be driven by the influence of wind and lagoon generated waves, or internal salinity differences within the lagoon. These currents are small within the lagoon (mean 15%), during the observation period, and have not been further investigated. It is suggested however, that the southeast trade winds would play a major role in driving these currents.

The unidirectional ocean to lagoon flow that occurs in the shallow passages, for all but spring low tides in the east of the atoll, can be explained through the interaction of tidal height and wave action, with the height of the reef crest. As the tide rises above the reef crest, waves incident at the reef break, reform (Gourlay 1990), travel over the reef and through the passage. These translatory currents comprise the bulk of the current accounted for by the residuals (Table 2). As the waves travel across the reef-flat, friction (induced by the reef flat morphology) slows the wave induced currents. This produces a build up of water at the reef crest which forms a hydraulic gradient from the reef crest to lagoon (Tait 1972). The movement of waves across the reef is still possible on the falling tide until the water height falls below that of the reef crest. The reversal in current direction in the eastern passages, around spring low tide, results from the interaction between tidal height at the reef crest and the height of the lagoonward sand bodies. As shown in Figure 9 the maximum height of the lagoonward sand body is greater than the reef crest. As the spring low tide falls below the level of the reef crest, water is ponded inside the sand apron with no connection to the deeper lagoon. A surface water gradient forms from lagoon to ocean producing a slow reefward flow. The magnitude of this reversing flow is small.

That tidal currents were observed within 1km of shallow passages, indicate that shallow passage currents have negligible effect in driving circulation beyond 1km of the passage exit. They may, however, be important in retarding and deflecting lagoon currents.

During the rising tide there is an opposition of currents entering the lagoon through shallow passages and the tidal currents penetrating the lagoon from the north-northwest toward the lee of the islands. The angle of opposition of these currents on the eastern side of the lagoon would indicate there is a deflection of rising tide water to the southeast. Net flow westward is the result of longer duration ebb flow which is reinforced by the continued flux of water through the shallow passages. Water behind South Island flows southward on the rising tide and west-southwest on the falling tide, as if of a semi-circular nature, driven by the shallow bathymetry and closed lagoon shoreline in this region (Figs. 2 and 3). Flow in the southwest is predominantly in the north-south direction with net movement northward. This net flow direction is thought result from the increased volume of water entering via the south passage and that volume of the lagoon prism that flows from the eastern side of the lagoon. The build up of water in the west of the lagoon is evacuated by the unidirectional northward flow along the western shoreline. Water may also be built up along this shoreline due to the southeast trade winds forcing surface water northwest. As the trade winds drop there may be a small flow of water toward the east to equalise this pressure gradient.

The northeastern passage experiences strong current reversals with tidal stage, whilst the northwestern passage exhibits a unidirectional and slow movement exiting the lagoon. The increased influx of water entering through the shallow passages for the duration of the tidal cycle must increase the length and or velocity of currents exiting the lagoon on the falling tide through these large passages. It is proposed that as the tidal wave sets from the east-northeast, the northeast passage is the major conduit for tidal inflow, while the northwest passage is dominated by net flow out of the lagoon (Fig. 2).

A general circulation model of the lagoon, therefore, has water entering and flowing down the eastern and central sections of the lagoon, on the rising tide; being deflected west inside South Island and flowing north up the central and western sides of the lagoon, and exiting the northwest pass during the falling tide (Fig. 10). The northeast pass also evacuates water from the lagoon on the falling tide. Results from vector plots (Figs. 2-5) identify a net flow within the lagoon which mirrors that of the falling (Fig. 10b) except for the northeast passage experiencing a westward flow. Tidal oscillation is superimposed on this net flow. There are two possible mechanisms of this net northwestward flow. First, the prevailing southeast wind may produce a small surface current, as seen in the southeast lagoon residual current (Fig. 7a). If this mechanism is important, ocean-lagoon exchange time will decrease during stronger wind conditions. Second, due to the ebb prism being greater than the flood prism, because of the continuous shallow passage input, the falling tide is of longer duration, producing a net movement in the vector plots toward the deep northwest passage. The unidirectional ocean to lagoon flux of water through the passages also retards the rising currents penetrating the lagoon from the north. Continued influx of water at slack tide and the falling tide may create a pressure head from the south and east toward the northwest and may also accelerate flow toward the northwest deep passage.

That circulation in the Cocos (Keeling) Islands lagoon is driven by tidal forces is consistent with other shallow lagoon studies in Pacific atolls (e.g. Stroup and Meyers 1974). While tidal forces dominate ocean-lagoon water exchange, the wave induced water flux through the shallow passages plays an important role in this exchange, especially during neap tides where shallow passage flux can represent 22% of the entire prism. Shallow passage water flux is also identified as a primary mechanism of lagoon-ocean water exchange by Atkinson et al. (1981) in Enewetak Atoll.

The flushing time of the lagoon is estimated at a minimum of 2.36 days and a maximum of 5.4 days for spring and neap tides. This time period is comparable with lagoons of similar size and depth including Aldabra atoll (Pugh and Rayner 1981) and Britomart lagoon, Great Barrier Reef (Wolanski and Pickard 1983). Fanning and Canton Atoll lagoons which have similar dimensions to the Cocos lagoon (15 km wide, 6 m deep) have far greater flushing time scales (50-95 days, Canton and <300 days Fanning) due primarily to the enclosed nature of the lagoon with few connections to the ocean.

CONCLUSION

The Cocos (Keeling) Islands are influenced by mixed mainly semi-diurnal tides. Tides in the shallow south of the lagoon and currents in south passage, lag those of the deeper northern lagoon and eastern passages.

The Cocos (Keeling) Islands lagoon circulation is tidally driven with strong tidal currents penetrating the lagoon from the northeastern passage to within 1km of the shallow passages. The tidal range has a significant impact on net flow direction in the east and southeastern sections of the lagoon. Shallow tidal constituents are important in the shallow southeastern section of the lagoon that is bordered by South island.

A general circulation model has been derived in which water entering the northeastern passage travels down the eastern shoreline of the lagoon, is deflected westward, and flows northwestward exiting through the northwest deep passage.

The role of wind was found to be small in driving lagoon circulation. Wind stress may contribute to the residual currents which produce a northwestward flow. However, these currents were weak within the lagoon.

Shallow passages experience unidirectional ocean to lagoon flow throughout neap tides and during spring tides in the south of the atoll. This unidirectional flow contributes to the net movement of lagoon water toward the northwest throughout the tidal cycle. Eastern passages display a reversal in current direction around spring low tides due to the interaction of tidal height at the reef crest and height of the sand apron lagoonward of the passage. Exposure of the sand apron crest produces a temporary reversed hydraulic gradient and current flow.

Shallow passage currents are dominated by translatory wave motion across the reef flat. Tidal currents contribute less than 50% to observed passage currents. The influence of shallow passage hydrodynamics on lagoon circulation is negligible. Shallow passage currents penetrate up to 1km lagoonward of the passage exit. These currents deflect water entering the deep lagoon to the southeast in the eastern side of the lagoon. Unidirectional passage flow increases the ebb prism and ebb tide current velocities.

Shallow passages were found to be important mechanisms for the exchange of water between ocean and lagoon with up to 15% (springtides) and 22% (neap tides) of total water entering the lagoon over a tidal cycle being transmitted through the shallow passages.

Flushing times of the Cocos lagoon were found to vary between 5.4 and 2.3 days for neap and spring tidal conditions respectively. These results were consistent with atoll lagoons of similar dimension and high degree of connection with the ocean.

REFERENCES

Andrews, J.C., and Pickard, G.L. 1990. The Physical Oceanography of Coral-Reef Systems. Chapter 2 In Dubinsky, Z. ed. Coral Reefs. p 11-48.

Atkinson, M., Smith, S.V. and Stroup, E.D. 1981. Circulation in Enewetak Atoll Lagoon. Limnology and Oceanography, 26:1074-1083.

Farrow, G.E. and Brander, K.M. 1971. Tidal Studies on Aldabra. Phil. Trans. Roy. Soc. Lond. B. 260: 93-121.

Foreman, M.G.G. 1979a. Manual for Tidal Heights Analysis and Prediction. Institute of Ocean Sciences, Patricia Bay Canada. Pacific Marine Science Report pp77-10.

Foreman, M.G.G. 1979b. Manual for Tidal Currents Analysis and Prediction. Institute of Ocean Sciences, Patricia Bay Canada. Pacific Marine Science Report pp78-6.

Gallagher, B.S., Shimada, K.M., Gonzales, F.I., Jr. and Stroup, E.D. 1971. Tides and Currents in Fanning Atoll Lagoon. Pacific Sci. 25: 191-205.

Gilmour, A.J. and Colman, R. 1990. A Pilot Study of the Outer Island Development Program Republic of Kiribati. Report to AIDAB on environmental studies, Kiribati.

Gourlay, M. 1990. Wave Set-up and Currents on Reefs. Cay Formation and Stability. Conference on Engineering in Coral Reef Regions, Magnetic Island Townsville Nov. 5-7.

Neumann, G. 1968. Ocean Currents. Elsevier Oceanography Series Volume 4. Elsevier publishing company, 351pp.

Platzman, G.W. 1984. Normal Modes of the World Ocean. Part IV: Synthesis of Diurnal and Semidiurnal Tides. J. Phys. Ocean. 14: 1532-1550.

Pond, S. and Pickard, G.L. 1983. Introduction to Dynamical Oceanography, Second Edition. Pergamon Press, 329pp.

Pugh, D.T. 1979. Sea Levels at Aldabra Atoll, Mombasa and Mahe, Western Equatorial Indian Ocean, Related to Tides, Meteorology and Ocean Circulation. Deep-Sea Res. 26: 237-258.

Pugh, D.T. and Rayner, R.F. 1981. The tidal regimes of three Indian Ocean atolls and some ecological implications. Estu. Cstl. Shelf Sci. 13: 389-407.

Smith, S.V. and Jokiel, P.L. 1978. Water Composition and Biogeochemical Gradients in the Canton Atoll Lagoon. Atoll Res. Bull. 221:15-54.

Stroup, E.D. and Meyers, G.A. 1974. The flood-tide jet in Fanning Island Lagoon. Pacific Sci. 28: 211-223.

Tait, R.J. 1972. Wave Set-up on Coral Reefs. J. Geophys. Res. 77: 2207-2211.

Tchernia, P. 1980. Descriptive Regional Oceanography. Pergamon Press.

von Arx, W.S. 1948. The Circulation Systems of Bikini and Rongelap Lagoons. Trans. Am. Geophys. Uni. 29: 861-870.

von Arx, W.S 1954. Circulation systems of Bikini and Rongelap Lagoons, Bikini and nearby atolls, Marshall Islands. U.S. Geol. Surv. Prof. Pap. 260-B: 265-273.

Wiens, H.J. 1962. Atoll Environment and Ecology. Yale University Press, New Haven, 532 pp.

Wolanski, E., and Pickard, G.L. 1983. Currents and Flushing of Britomart Reef Lagoon. Coral Reefs 2: 1-8.

Table 1: Harmonic analysis of lagoon tides, centimetres and degrees in relation to Greenwhich. Major tidal constituents at the permanent Home Island tide gauge and temporary location in South Passage. Symbols indicate tidal properties of amplitude (a) and phase (g). Due to the short length of record from the temporary tide gauge (20 days) the N_2 constituent was unable to be resolved.

Constituents	Frequency (hours)	Home Island a (cm)	Home Island g(deg)	South Passage a(cm)	South Passage g(deg)
MSF	354.37	6.02	60.16	7.21	237.33
O_1	25.82	7.82	236.50	8.23	256.37
K_1	23.93	12.19	259.44	10.29	282.27
N_2	12.65	10.92	118.03	——	——
M^2	12.42	29.39	140.84	25.02	149.35
S_2	12.00	14.26	186.36	5.58	186.48
M_4	6.21	0.21	205.31	3.92	244.04

Table 2: Tidal current constituents at M2 (12.42 hrs) and K1 (23.93 hrs) frequencies. The symbols indicate current ellipse properties of semi–major axis length (a), semi–minor axis length (b), phase (g) and orientation (θ) measured anticlockwise from east. Residual, percentages of the orthogonal components of velocity (northing – n and easting – e) indicate the percentage of observed currents not able to be accounted for by tidal forces.

Mooring	M_2 a (cm/s)	M_2 b (cm/s)	M_2 g (deg)	M_2 θ (deg)	K_1 a (cm/s)	K_1 b (cm/s)	K_1 g (deg)	K_1 θ (deg)	Residuals n (%)	Residuals e (%)
E Lagoon	11.36	0.56	219.36	146.98	2.61	0.17	325.44	142.01	13.8	5.0
SE Lagoon	7.03	3.68	216.32	117.84	2.49	0.99	338.25	140.17	17.2	27.0
SW Lagoon	16.95	1.03	219.09	105.81	5.56	0.03	330.13	111.03	12.1	19.1
South Pass	7.60	2.11	337.79	263.88	4.13	0.80	235.32	82.21	46.4	29.9
East Pass	5.15	1.13	226.33	29.47	2.19	0.18	181.89	210.49	38.96	52.8

Table 3: Lagoon volumes and tidal prism calculations for the Cocos (Keeling) Islands Lagoon. Low–High = low to high tide shallow passage flux.

	Lagoon Volume ($M^3 \times 10^6$) High Tide	Lagoon Volume ($M^3 \times 10^6$) Low Tide	Tidal Prism ($M^3 \times 10^6$)	Shallow Passage Flux ($M^3 \times 10^6$) Low–High	Shallow Passage Flux ($M^3 \times 10^6$) High–Low	Total ($M^3 \times 10^6$)
SprinTides	612.5	505.5	107	10.5	5.1	15.6
Neap Tides	571.9	524.5	47	8.0	3.6	11.6

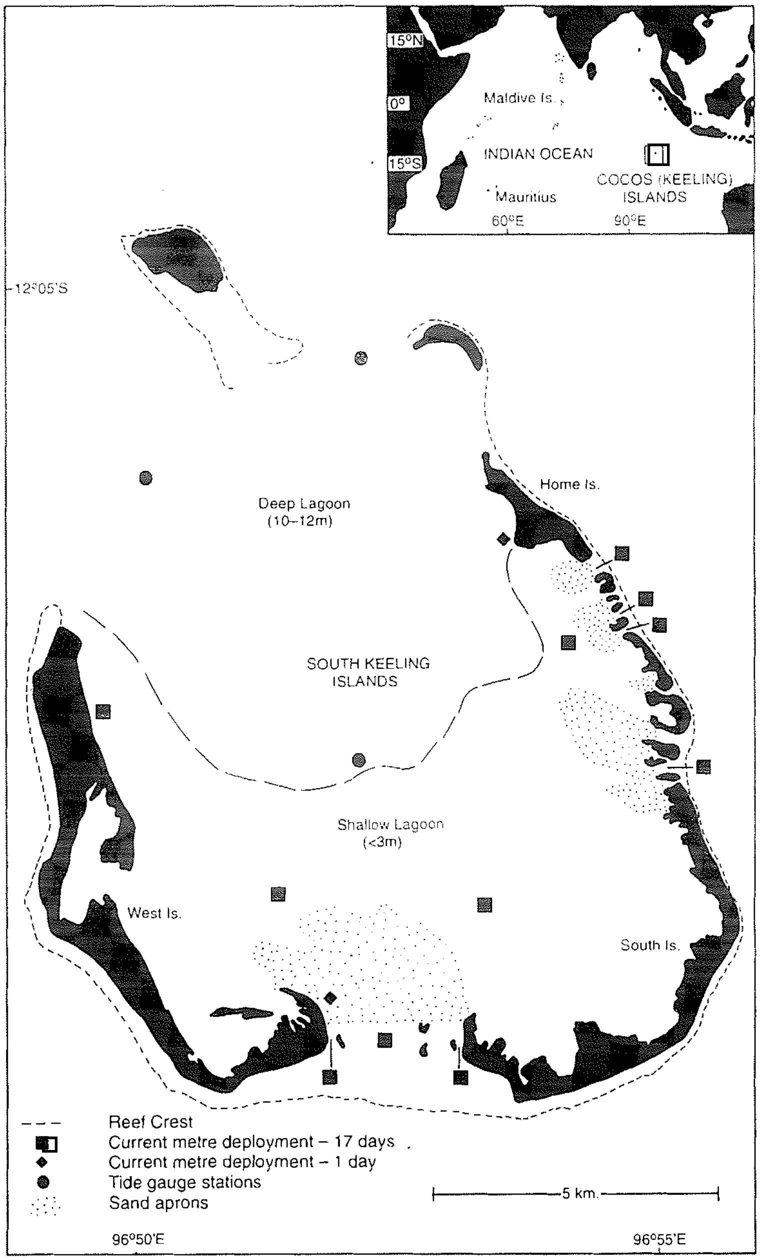

Figure 1. Field and Instrument location

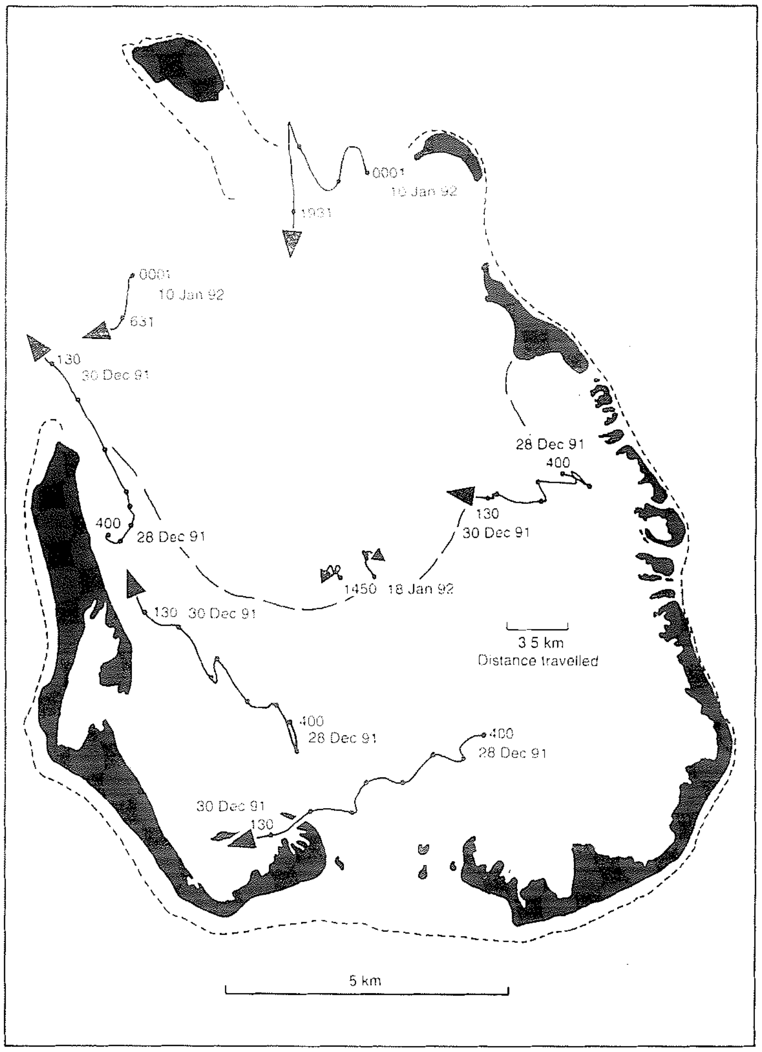

Figure 2. Lagoon progressive vector plots, neap tide. The four shallow lagoon locations show a 48 hour period starting 28/12/91 at 4am (low tide). The northwest passage is a 12 hour record and the northeast and mid lagoon locations are 24 hour records of current speed and direction.

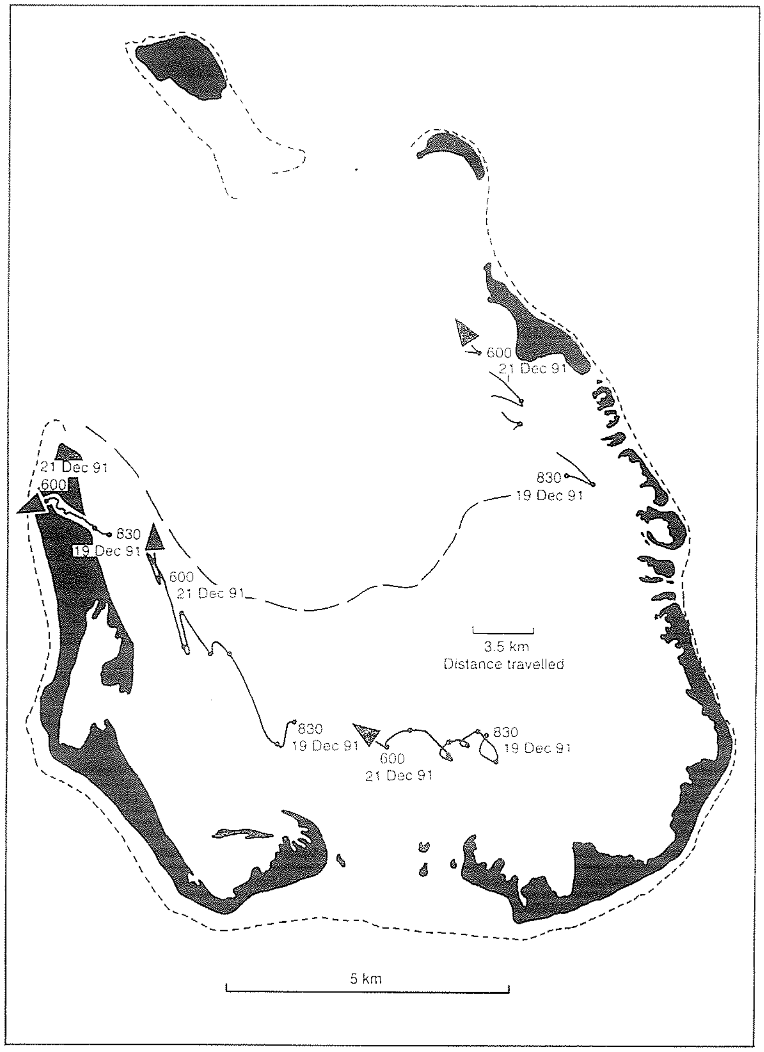

Figure 3. Lagoon progressive vector plots, spring tide. Each location displays a 48 hour period beginning 19/12/91 at 830am (low tide).

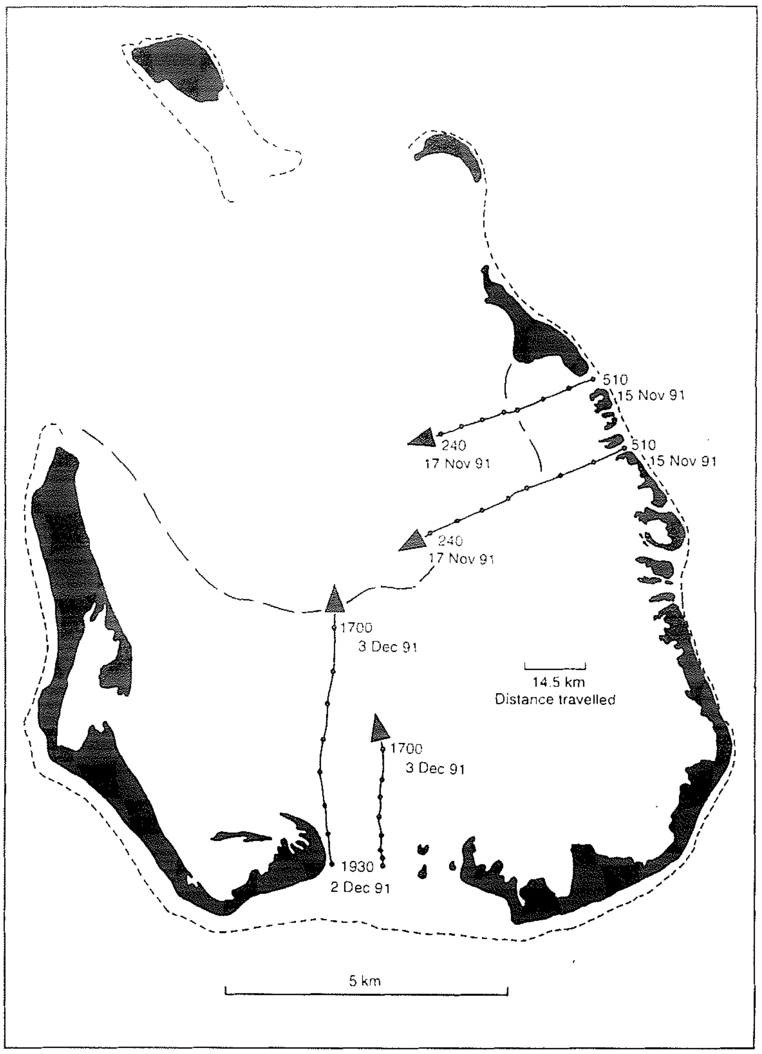

Figure 4. Shallow passage progressive vector plots, neap tide. 48 hour periods starting at low tide on the 15/11/91 at 510am in the eastern passages and 1/12/91 at 730pm in the southern passages.

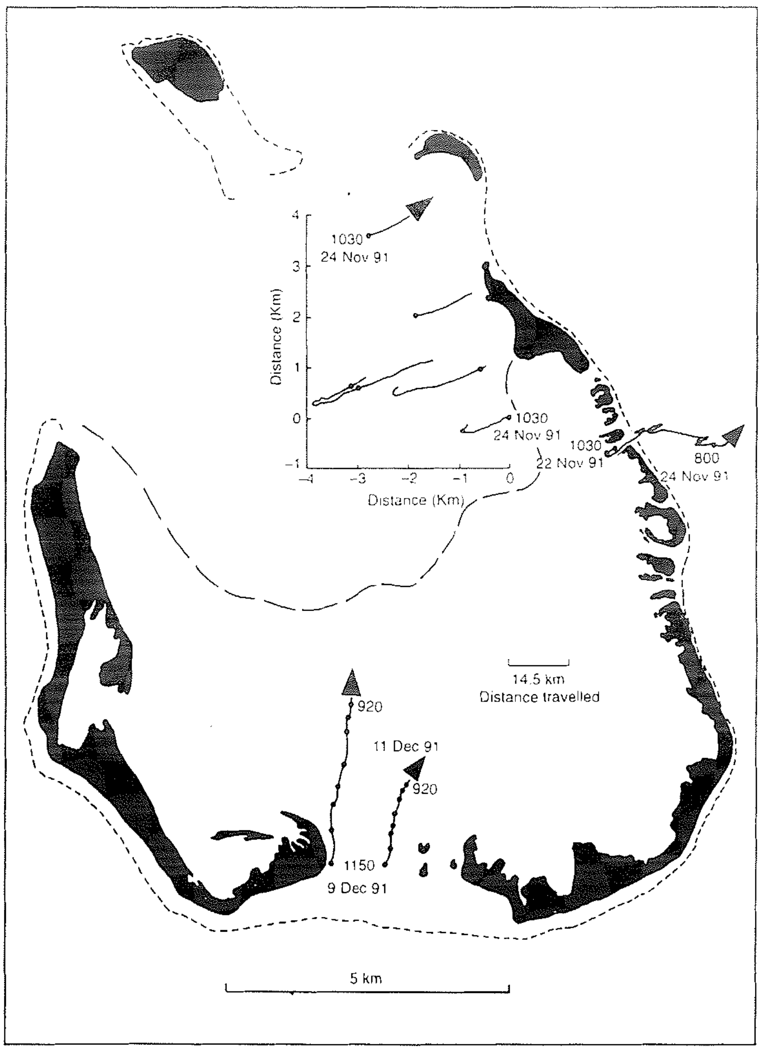

Figure 5. Shallow passage progressive vector plots, spring tide. 48 hour periods starting at low tide on the 22/11/91 at 1030am in the eastern passages and 9/12/91 at 1150am in the southern passages.

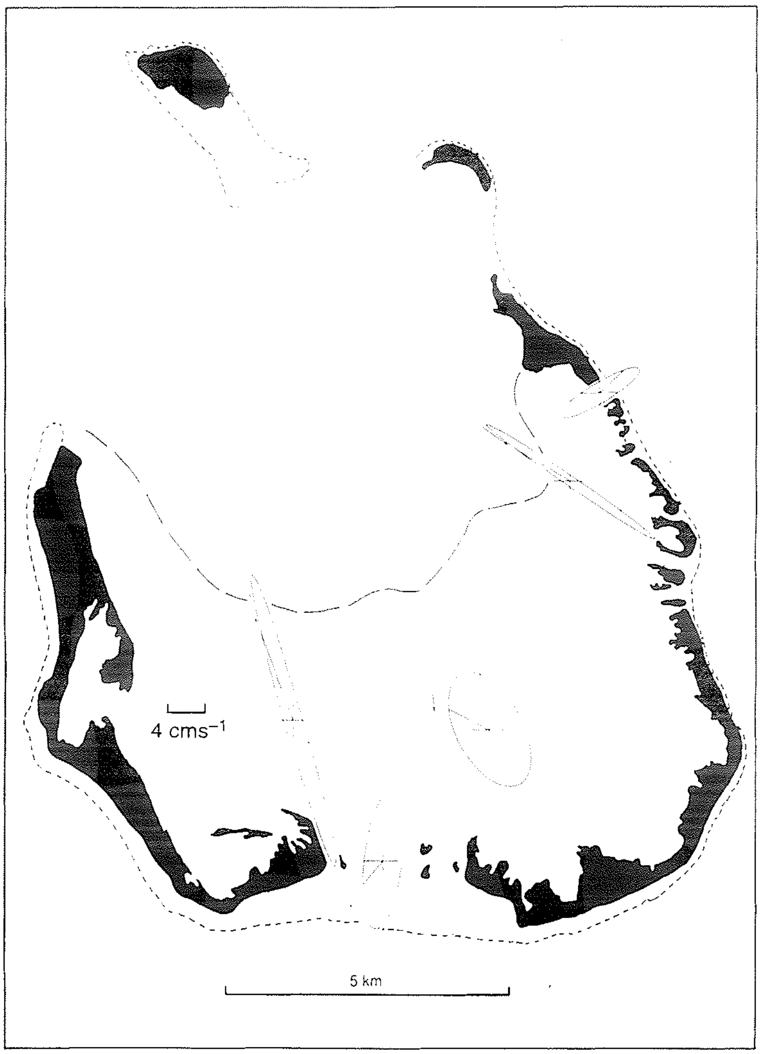

Figure 6. M2 tidal current ellipses for the shallow lagoon and passages. All display anti–clockwise rotation.

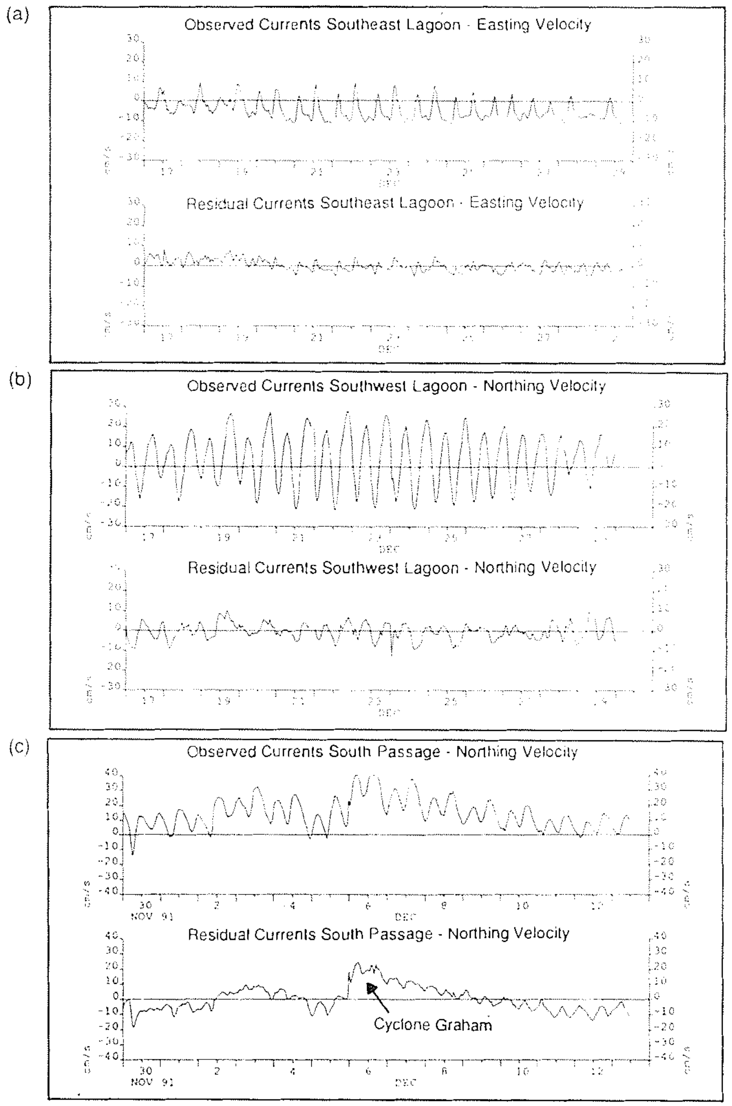

Figure 7. Observed and residual current information for selected sites. Residuals are derived by subtracting tidal current components from the observed current record. (a) Southeastern lagoon Showing the easting component of velocity. Negative values indicate flow to the west. (b) South west lagoon, showing the northing component of velocity. Negative values indicate flow to the south. (c) Southern passage, northing component of velocity.

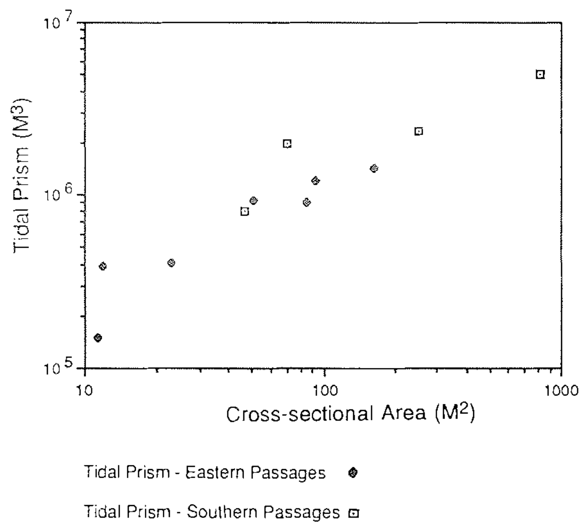

Figure 8. Spring tidal prism vs cross–sectional area (at MSL) relationship for the shallow passages.

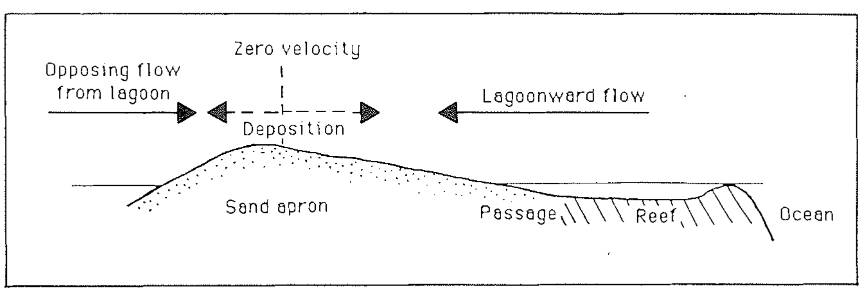

Figure 9. Relative height of sand apron and reef crest, eastern side of the atoll. The opposition of currents entering the lagoon via the deep passes and shallow passages is also shown.

(A) Rising tide

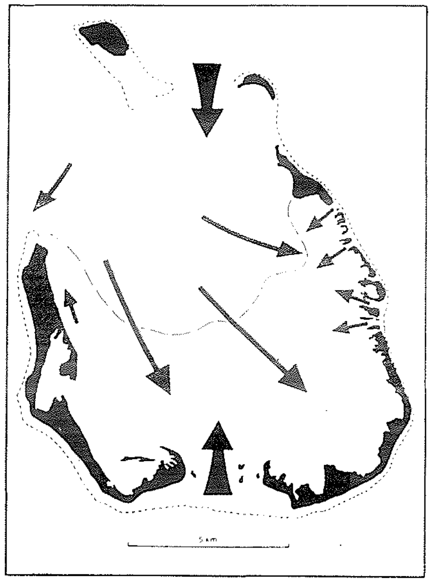

(B) Falling tide

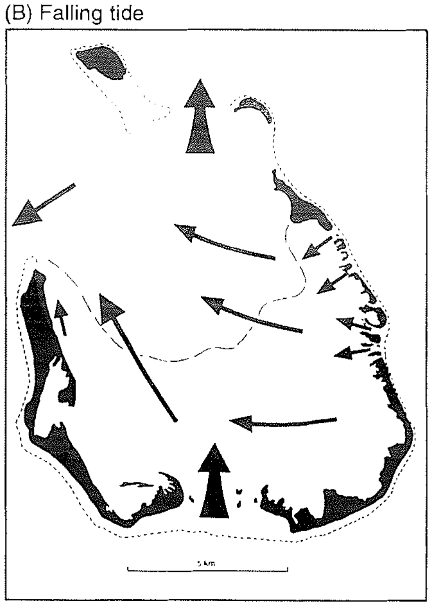

Figure 10. General circulation of the Cocos (Keeling) Islands lagoon on the rising (A) and falling (B) tide.